

Many-body entanglement in a topological chiral ladder

Ritu Nehra,¹ Devendra Singh Bhakuni,¹ Suhas Gangadharaiah,¹ and Auditya Sharma^{1,*}

¹*Department of Physics, Indian Institute of Science Education and Research, Bhopal, India*

We find that the topological phase transition in a chiral ladder is characterized by dramatic signatures in many body entanglement entropy between the legs, close to half-filling. The value of entanglement entropy for various fillings close to half-filling is identical, at the critical point, but splays out on either side, thus showing a sharp signature at the transition point. A second signature is provided by the change in entanglement entropy when a particle is added (or subtracted) from half-filling which turns out to be exactly $-\log 2$ in the trivial phase, but zero in the topological phase. A microscopic understanding of tendencies to form singlets along the rungs in the trivial phase, and along the diagonals in the topological phase, is afforded by a study of concurrence. At the topological phase transition the magnitude of the derivative of the average concurrence of all the rungs shows a sharp peak. Also, at the critical point, the average concurrence is the same for various fillings close to half-filling, but splays out on either side, just like entanglement entropy.

Topological states of matter [1, 2] have been at the centre of physics research in the last decade or so. One of the reasons for excitement has been the apparent simplicity of the models involved underneath which rich physics lies, and continues to be unearthed. Topologically significant states are often accompanied by the presence of ‘edge states’ with metallic properties while the bulk is gapped and insulating. It has been long realized that entanglement in the many-body ground state can be a useful diagnostic for topological order. While the scaling to leading order of entanglement entropy is governed by the famous ‘area law’ [3, 4], it is the subleading part that is linked with topological order and has now come to be known as topological entanglement entropy [5–7]. A finer tool, namely the entanglement spectrum has also been widely used [8–14].

In this Letter, we point out that entanglement in the many body ground state, when considered in a comparative study of various fillings close to half-filling may show a dramatic signature at a topological phase transition. We choose a specific system, namely a two leg chiral ladder, that has received a lot of attention in recent times [15–17], but not from an entanglement perspective. This simple system turns out to be rich with a Meissner to vortex phase transition, and in the presence of diagonal hopping, a trivial-to-topological phase transition. The study of entanglement in the many body and single particle ground states in this system offers useful fresh insights for not only the topological phase transition, but for the Meissner to vortex phase transition as well. In order to compute entanglement entropy in the many body ground states of these systems, we exploit the clever techniques of Peschel and co-workers [18, 19].

A further feature in our work is an investigation into the role of concurrence [20, 21], a measure of two-site entanglement, whose study allows us to track microscopic quantum correlations, and how they alter at the topological phase transition. Any study of entanglement involves the specification of subsystem and its complement; in the ladder system, a natural subsystem to work with is one

of the legs. With such a choice, it is of interest to understand not only the entanglement content between the two full legs, but also to consider the entanglement in each rung separately, where concurrence proves to be handy.

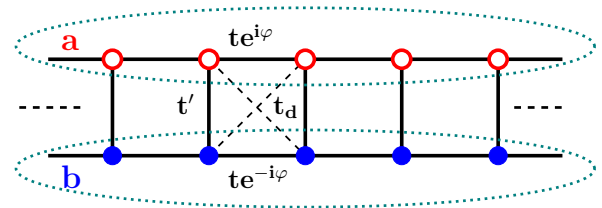


FIG. 1: The ladder system consists of two legs **a** and **b** with uniform magnetic flux ϕ per plaquette. The horizontal division for the computation of entanglement entropy, is delineated.

The system consists of a two-leg ladder of non-interacting fermions subjected to a uniform magnetic flux ϕ per plaquette - a schematic diagram is given in Fig. 1. The Hamiltonian can be written as [15, 16, 22]

$$H = -t \sum_{\ell} (e^{i\phi} a_{\ell+1}^{\dagger} a_{\ell} + e^{-i\phi} b_{\ell+1}^{\dagger} b_{\ell}) - t' \sum_{\ell} a_{\ell}^{\dagger} b_{\ell} - t_d \sum_{\ell} (a_{\ell}^{\dagger} b_{\ell+1} + b_{\ell}^{\dagger} a_{\ell+1}) + H.c., \quad (1)$$

where the operator $a_{\ell}(b_{\ell})$ is the annihilation operator at site ℓ in the right(left) leg of the ladder. The parameters t , t' and t_d are the hopping amplitudes along the legs of the ladder, along the rungs of the ladder without magnetic field and along the diagonals of each plaquette, respectively, and L is the length of the ladder. It is useful to define $\xi = \frac{t'}{2t}$, $\xi_d = \frac{t_d}{t}$. Using an appropriate gauge, the magnetic field is absorbed into the hopping term ($t \rightarrow te^{i\phi}$, $\phi = \phi/2$) by Peierls substitution.

The ladder model shows a trivial-to-topological phase transition for any general ϕ , which is signaled by a change

in winding number. As shown in Fig. 2, there is a change in winding number from 0 to 1 on increasing ξ_d while keeping φ constant. The Fourier transform of Eq. 1 can be cast into the general form of a 2×2 matrix in terms of Pauli matrices as $\mathcal{H}(k) = d_0 I + d_x \sigma_x + d_y \sigma_y + d_z \sigma_z$, where $d_0 = -\cos \varphi \cos k$, $d_x = -\xi - \xi_d \cos k$, $d_y = 0$, and $d_z = -\sin \varphi \sin k$. Here, only d_x and d_z contribute to the winding number calculation. Eliminating k , we have the trajectory

$$\left(\frac{d_x + \xi}{\xi_d}\right)^2 + \left(\frac{d_z}{\sin \varphi}\right)^2 = 1, \quad (2)$$

from which the winding number around the origin is computed (Fig. 2). So, there is a trivial-to-topological phase

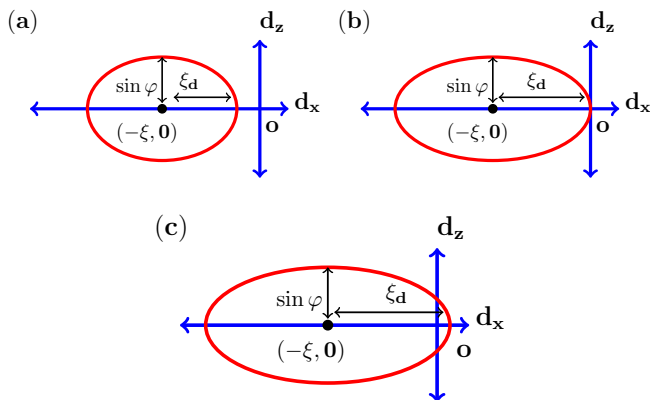


FIG. 2: The change in winding number with respect to change in ξ_d : (a) Trivial phase $\xi_d < \xi$, (b) the critical point $\xi_d = \xi$, and (c) the topological phase $\xi_d \geq \xi$.

transition at $\xi = \xi_d$ for any φ ; the only role of φ is to alter the minor axis length in the winding number calculation.

The most widely used quantity to measure entanglement in a pure state of a bipartite system is entanglement entropy, which is nothing but the von Neumann entropy of the subsystem. In general, this involves the computation of the reduced density matrix followed by diagonalization - often a daunting task for many body states, since the size of the reduced density matrix typically scales exponentially with the system size. However, for many body eigenstates of *quadratic fermionic Hamiltonians*, the correlation matrix approach developed by Peschel and co-workers [18], facilitates this computation by reducing the diagonalization problem to order of the system size. We adopt this approach to study entanglement in the many-body ground state of our system. We show that the entanglement contained in the many body ground state, close to half-filling reveals striking features for the topological phase transition. The overall correlation matrix for the ladder is given by

$$C_{2L \times 2L} = \begin{bmatrix} \langle a_m^\dagger a_n \rangle & \langle a_m^\dagger b_n \rangle \\ \langle b_m^\dagger a_n \rangle & \langle b_m^\dagger b_n \rangle \end{bmatrix}, \quad (3)$$

where $m, n = 1, 2, \dots, L$. To compute entanglement, one first selectively pulls out the part of the correlation matrix which relates to the subsystem of interest and diagonalizes this subsystem correlation matrix. The entanglement entropy of the subsystem with respect to its complement is given in terms of the eigenvalues C_i of the subsystem correlation matrix by

$$S = - \sum_i (C_i \ln C_i + (1 - C_i) \ln(1 - C_i)). \quad (4)$$

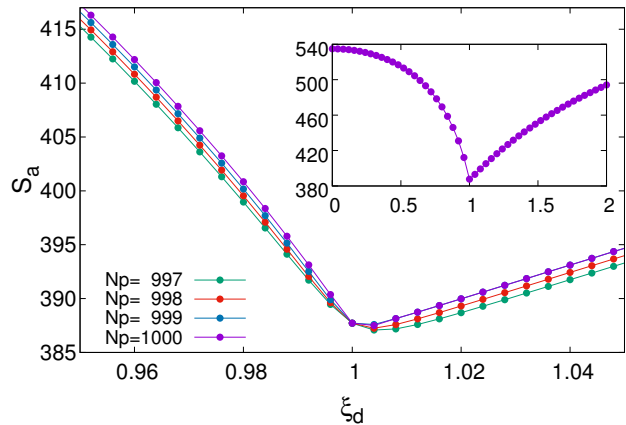


FIG. 3: The subsystem entanglement entropy (S_a) for the horizontal cut (Fig. 1) as a function of ξ_d , close to half-filling. Number of rungs $L = 1000$, $\varphi = \frac{\pi}{2}$ and $\xi = 1$ with open boundary conditions(OBC) imposed. S_a takes on the same value for various fillings close to half-filling at the critical point. S_a attains a minimum right after the topological phase transition ($\xi_d = 1$). The inset shows only the data for half-filling in an extended region.

Here we focus on the entanglement between the two legs of the ladder as shown in Fig. 1. The ladder model lends itself naturally to the horizontal division. Most studies of entanglement in chains (of the SSH model [23], for example) have looked at the vertical division, where a horizontal division does not exist. The supplementary section does contain a discussion of entanglement in the ladder model but with the other natural division, namely the vertical division. In the absence of diagonal hopping, when ξ dominates, the rungs of the system tend to form singlets. Furthermore, in the limit where the legs hopping t goes to zero, entanglement entropy goes to $N_p \log 2$, where N_p is the number of particles, and $\log 2$ is the contribution from each singlet. As the legs hopping and the magnetic flux contribution along the legs of the ladder are turned on, a deviation from the value $N_p \log 2$ is seen, although it continues to be of this order of magnitude. Fig. 3 shows the variation of entanglement entropy as a function of diagonal hopping, in the vicinity

of half-filling. In the trivial phase ($\xi_d < \xi$), as the diagonal hopping is increased the singlets along the rungs are systematically weakened, and therefore the entanglement entropy decreases steadily. However, for ($\xi_d > \xi$) edge states appear, and form singlets (evidence for this comes from a study of concurrence which appears later). This causes the entanglement entropy to increase when ξ_d is increased in the topological phase. In addition, the large values of ξ_d cause singlets to be formed along the diagonals, which once again, in the limit of very large ξ_d yield a total entanglement entropy of $N_p \log 2$, although from a different mechanism here. The topological phase transition is thus signalled by the entanglement entropy attaining a value independent of filling in the vicinity of half-filling. The entanglement entropy also attains a minimum soon after the topological phase is entered; this minimum seems to be directly correlated with the gap in the spectrum closing.

It is also insightful to study the entropy difference when a particle is either added or removed from the half-filled state:

$$\Delta S = S_{\text{hf}+1} - S_{\text{hf}}. \quad (5)$$

Fig. 4 shows that in the topological phase ΔS goes to zero, whereas in the trivial phase, ΔS is $-\log 2$. The $-\log 2$ difference would be expected in the limit of the legs hopping going to zero, because the half-filled state can then be thought of as N_p singlets. The removal or addition of one particle would then result in the destruction of entropy equal to that of one singlet. But, it is remarkable that this difference remains exactly $-\log 2$, even in the presence of legs hopping and flux. In the topological phase, the limit of large but finite ξ_d is a useful reference. At half-filling, exactly one of the edge states is occupied, and this contributes zero to the entanglement, while the remaining electrons form singlets along the diagonals. When one particle is added to this state, it lands in the other edge, which also contributes nothing to the entanglement, and thus ΔS would be zero. We see from Fig. 4 that this feature is exact throughout the topological phase for $\varphi = \pi/2$. For other values of φ though, we see that as one approaches the critical point within the topological phase, the edge states do contribute to the entanglement, thus causing ΔS to overshoot zero. This seems to be related to the edge states being not completely localized at the edges, when φ is decreased.

In order to acquire a finer understanding of the nature of the many body ground state wavefunctions, in various phases of the system, it is useful to study two-site entanglement. An excellent measure for this purpose is concurrence [21, 24–28]. One nice feature of concurrence is that for a number conserving Hamiltonian, the two-site concurrence is readily obtained, regardless of whether the density matrix is pure or mixed. This follows from the structure of the reduced density matrix for two sites i

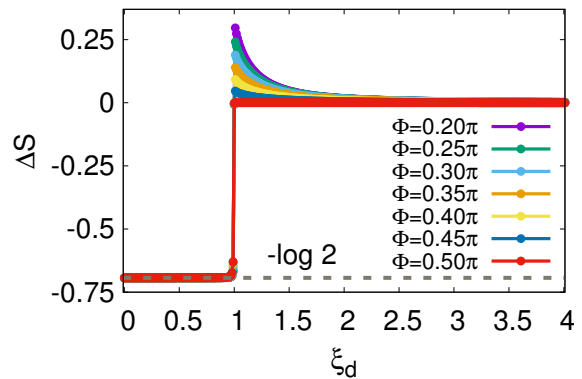


FIG. 4: ΔS as a function of ξ_d under open boundary conditions (OBC) for various φ . $\xi = 1.0$, $L = 1000$.

and j (with $i < j$), which can be written as

$$\rho_{ij} = \begin{bmatrix} u_{ij} & 0 & 0 & 0 \\ 0 & w_{1ij} & z_{ij}^* & 0 \\ 0 & z_{ij} & w_{2ij} & 0 \\ 0 & 0 & 0 & v_{ij} \end{bmatrix}, \quad (6)$$

where, $u_{ij} = \langle (1-n_i)(1-n_j) \rangle$, $w_{1ij} = \langle (1-n_i)n_j \rangle$, $w_{2ij} = \langle n_i(1-n_j) \rangle$, $v_{ij} = \langle n_i n_j \rangle$ and $z_{ij} = \langle c_j^\dagger c_i \rangle$. The concurrence is then given by

$$\mathcal{C} = 2 \max(0, |z| - \sqrt{uv}). \quad (7)$$

However, in the noninteracting framework, \mathcal{C} can be directly calculated from the subsystem correlation matrix of the two sites. Employing Wick's theorem one can decompose the four point correlators into two point correlators; the non zero elements of the reduced density matrix ρ_{ij} are then simplified in terms of the correlation matrix.

The concurrence between two sites is maximum and equal to unity when they form a singlet. For the ladder model, we can expect that the system at half-filling, has a tendency to form singlets in each rung when the rungs hopping is high and when the diagonal hopping is small. As the diagonal hopping is increased, the tendency to form singlets along the diagonals would be enhanced. The study of concurrence reinforces these expectations. Fig. 5(a) shows the concurrence between the two sites on a rung, averaged over all rungs, as a function of ξ_d . Also included in the same figure is the concurrence between the sites on a diagonal, averaged over all diagonals of the ladder. It is seen that for large ξ_d , the rungs concurrence drops to zero, whereas for small ξ_d , the diagonal concurrence is zero. This type of a feature has been reported in the literature in the context of the SSH model [24] and has been called 'sudden-death of concurrence' - it is a quantum information effect, and the value of ξ_d at which this change happens does not seem to have any significance for the phases of the model. Moreover the

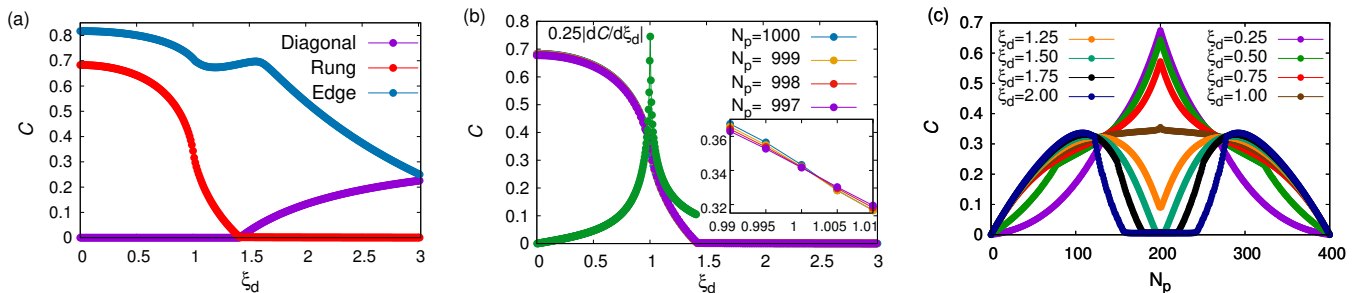


FIG. 5: (a) Average concurrence of diagonals, rungs and edge states of system with varying ξ_d for half filling. (b) Average concurrence of rungs with ξ_d near half filling. Also, the derivative of concurrence (green) featuring the trivial-to-topological transition. Inset shows a similar feature as Fig. 3 for average rungs concurrence. (c) Average concurrence of rungs as a function of filling, for various diagonal hopping. In all the figures, the parameters are $\xi = 1.0$, $L = 1000$ and $\varphi = \frac{\pi}{2}$ and open boundary conditions are imposed.

ξ_d values at which the change happens for the rungs and the diagonal concurrence, are close, but not identical.

A study of the concurrence between the edge sites is profitable for an investigation into the role of quantum correlations within the edge states in the topological phase. We notice that this shows a sharp change at the topological phase transition point $\xi_d = \xi$. For $\xi_d \geq \xi$, when the topological phase has just been entered, although the overall concurrence between rungs continues to decrease, we observe that the concurrence in the edge states increases in a brief range. This suggests that the edge states when they have just formed have singlet-like nature; however as the diagonal rungs are cranked up, this character steadily decreases as the diagonals become more and more singlet-like. The point at which the edge-state concurrence begins once again to decrease seems to be connected to the appearance of an enhanced density of states in the topological region, which is discussed in the supplementary section.

It is also illuminating to study concurrence in the rungs, for a range of fillings close to half-filling. The inset of Fig. 5(b) shows that at the topological phase transition, the average rungs concurrence, similar to entanglement entropy, also attains the same value for various fillings close to half-filling, and nicely splays out on either side of the topological phase transition. The derivative of concurrence shows a sharp feature at the topological phase transition. Concurrence as a diagnostic at a phase transition has been used in the SSH model [24], the Harper model [28], and in spin chains [29]. Fig. 5(c) looks at the dependence of rungs concurrence, as a function of filling, both in the trivial and the topological phases. We see that in the trivial phase, concurrence has a peak at half-filling, whereas this dramatically becomes a dip, as soon as the topological phase is entered. Furthermore, in the limit of very large diagonal hopping, this dip becomes a broad basin, close to half-filling. At the topological phase transition, it is an almost entirely smooth curve,

except for a tiny peak at half-filling which comes from the edge states - we have verified that the corresponding model with periodic boundary conditions shows a completely smooth curve, indicating that the tiny peak must indeed be a consequence of the edge states.

To summarize, many body entanglement close to half-filling can provide dramatic signatures at a topological phase transition. We show this by considering the specific system of a chiral ladder. The entanglement entropy between the legs of the ladder is independent of filling, close to half-filling, if one is exactly at the topological critical point, whereas this independence is lost on either side of the transition. A similar feature is also shown by average concurrence in all the rungs of the ladder. The magnitude of the derivative of this concurrence has a dramatic peak at the transition point. Addition or subtraction of a particle at half-filling can lead to either a precise change of $-\log 2$ in entanglement entropy in the trivial phase, or no change in the topological phase, due to the presence of edge states. In this Letter, we have emphasized the usefulness of considering the entanglement entropy between the two legs of the ladder in the many-body eigenstates. A study of single-particle entanglement with the same division captures the Meissner to vortex phase transition; these details can be found in the supplementary section. The study of entanglement entropy in the many-body ground state, but with a vertical division of the subsystem provides further insights into the topological phase transition - this too can be found in the supplementary section. Our work opens up the question of how general these features of many-body entanglement are for topological phase transitions. Recent work [17] shows that an electric field in this system can lead to chiral Bloch oscillations. Whether this can give rise to special entanglement effects is worth investigating.

A.S is grateful to SERB for the startup grant (File Number: YSS/2015/001696).

* auditya@iiserb.ac.in

- [1] B. A. Bernevig and T. L. Hughes, *Topological insulators and topological superconductors* (Princeton University Press, 2013).
- [2] J. K. Asbóth, L. Oroszlány, and A. Pályi, *A short course on topological insulators: Band structure and edge states in one and two dimensions*, Vol. 919 (Springer, 2016).
- [3] M. B. Hastings, *Journal of Statistical Mechanics: Theory and Experiment* **2007**, P08024 (2007).
- [4] J. Eisert, M. Cramer, and M. B. Plenio, *Rev. Mod. Phys.* **82**, 277 (2010).
- [5] A. Kitaev and J. Preskill, *Physical review letters* **96**, 110404 (2006).
- [6] M. Levin and X.-G. Wen, *Physical review letters* **96**, 110405 (2006).
- [7] H.-C. Jiang, Z. Wang, and L. Balents, *Nature Physics* **8**, 902 (2012).
- [8] H. Li and F. D. M. Haldane, *Physical review letters* **101**, 010504 (2008).
- [9] S. Ryu and Y. Hatsugai, *Physical review B* **73**, 245115 (2006).
- [10] N. Bray-Ali, L. Ding, and S. Haas, *Physical Review B* **80**, 180504 (2009).
- [11] S. T. Flammia, A. Hamma, T. L. Hughes, and X.-G. Wen, *Physical review letters* **103**, 261601 (2009).
- [12] R. Thomale, A. Sterdyniak, N. Regnault, and B. A. Bernevig, *Physical review letters* **104**, 180502 (2010).
- [13] F. Pollmann, A. M. Turner, E. Berg, and M. Oshikawa, *Physical review b* **81**, 064439 (2010).
- [14] E. Prodan, T. L. Hughes, and B. A. Bernevig, *Physical review letters* **105**, 115501 (2010).
- [15] D. Hügél and B. Paredes, *Physical Review A* **89**, 023619 (2014).
- [16] M. Atala, M. Aidelsburger, M. Lohse, J. T. Barreiro, B. Paredes, and I. Bloch, *Nature Physics* **10**, 588 (2014).
- [17] Y. Zheng, S. Feng, and S.-J. Yang, *Physical Review A* **96**, 063613 (2017).
- [18] I. Peschel, *Brazilian Journal of Physics* **42**, 267 (2012).
- [19] X. Chen and E. Fradkin, *Journal of Statistical Mechanics: Theory and Experiment* **2013**, P08013 (2013).
- [20] S. Hill and W. K. Wootters, *Physical review letters* **78**, 5022 (1997).
- [21] W. K. Wootters, *Physical Review Letters* **80**, 2245 (1998).
- [22] E. Orignac and T. Giamarchi, *Physical Review B* **64**, 144515 (2001).
- [23] J. Sirker, M. Maiti, N. Konstantinidis, and N. Sedlmayr, *Journal of Statistical Mechanics: Theory and Experiment* **2014**, P10032 (2014).
- [24] J. Cho and K. W. Kim, *Scientific reports* **7**, 2745 (2017).
- [25] S.-S. Deng, S.-J. Gu, and H.-Q. Lin, *arXiv preprint quant-ph/0406078* (2004).
- [26] P. Zanardi and X. Wang, *Journal of Physics A: Mathematical and General* **35**, 7947 (2002).
- [27] A. P. Majtey, P. A. Bouvrie, A. Valdés-Hernández, and A. R. Plastino, *Phys. Rev. A* **93**, 032335 (2016).
- [28] A. Lakshminarayan and V. Subrahmanyam, *Physical Review A* **67**, 052304 (2003).
- [29] A. Osterloh, L. Amico, G. Falci, and R. Fazio, *Nature* **416**, 608 (2002).

Supplementary material for “Many-body entanglement in a topological chiral ladder”

Ritu Nehra,¹ Devendra Singh Bhakuni,¹ Suhas Gangadharaiah,¹ and Auditya Sharma¹

¹*Department of Physics, Indian Institute of Science Education and Research, Bhopal, India*

I. LADDER HAMILTONIAN

Since the Hamiltonian is translationally invariant along the legs, its momentum space version reads

$$H = 2t \sum_k c_k^\dagger \mathcal{H}(k) c_k, \quad (1)$$

where

$$\mathcal{H}(k) = \begin{bmatrix} -\cos(\varphi - k) & -\xi - \xi_d \cos k \\ -\xi - \xi_d \cos k & -\cos(\varphi + k) \end{bmatrix}, \quad (2)$$

with $c_k^\dagger = [a_k^\dagger \ b_k^\dagger]$, $c_k = \begin{bmatrix} a_k \\ b_k \end{bmatrix}$, $\xi = \frac{t'}{2t}$, $\xi_d = \frac{t_d}{t}$. The dispersion consists of two bands with E_+ (E_-) being the energies of higher (lower) energy band:

$$E_{\pm}(k) = -\cos \varphi \cos k \pm \sqrt{(\xi + \xi_d \cos k)^2 + \sin^2 \varphi \sin^2 k}. \quad (3)$$

The corresponding eigenvectors are

$$\Gamma_k^\dagger |0\rangle = \frac{1}{N} \left((\xi + \xi_d \cos k) a_k^\dagger + Y b_k^\dagger \right) |0\rangle \quad (4)$$

$$\Omega_k^\dagger |0\rangle = \frac{1}{N} \left(-Y a_k^\dagger + (\xi + \xi_d \cos k) b_k^\dagger \right) |0\rangle, \quad (5)$$

where $\Gamma_k^\dagger, \Omega_k^\dagger$ are new creation operators for the lower (E_-) and higher (E_+) energy bands respectively, with $Y = \sqrt{(\xi + \xi_d \cos k)^2 + \sin^2 \varphi \sin^2 k} - \sin \varphi \sin k$ and $N = \sqrt{(\xi + \xi_d \cos k)^2 + Y^2}$ is the normalization constant.

II. THE VORTEX TO MEISSNER PHASE TRANSITION

Entanglement in the single-particle states provides useful signatures of the vortex-to-Meissner phase transition [1, 2], which will be described in this section.

A. No diagonal hopping

In the absence of diagonal hopping ($t_d = 0$), there are two parameters: one is the uniform magnetic field and the other is ξ . For a constant ξ and increasing φ , the dispersion curve shows a phase transition from the Meissner to the vortex phase at a certain critical value of φ . From the dispersion curves in Fig. 1, it can be seen that the lower energy band of the system possesses two

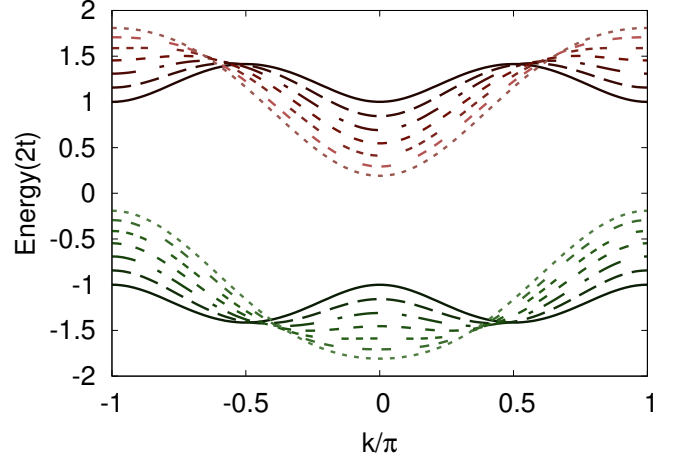


FIG. 1: Lower energy band (green color) and higher energy band (red color) for the ladder system with the parameters $\xi = 0.5$, $\xi_d = 0$. Decreasing intensity of color (length of dots) corresponds to decreasing φ starting from 0.5π , in units of 0.05 down to 0.2π .

minima at $\pm k_g$ which become one minimum at $k = 0$, on decreasing φ below a critical value φ_c . The critical value φ_c is obtained by minimizing the lower band energy $E_-(k)$ with respect to k , and demanding that $k_g \neq 0$. This yields

$$\varphi_c = \cos^{-1} \left(\frac{-\xi + \sqrt{\xi^2 + 4}}{2} \right) \quad (6)$$

$$\sin k_g = \pm \sqrt{\sin^2 \varphi_c - \cot^2 \varphi_c \xi^2}. \quad (7)$$

This phase transition is captured by other quantities like the chiral current [1]. The currents in the two legs are

$$J_a = \sum_l J_{a_l} = \frac{i}{2} \sum_l \langle e^{i\varphi} a_l^\dagger a_{l-1} - e^{-i\varphi} a_{l-1}^\dagger a_l \rangle \quad (8)$$

$$J_b = \sum_l J_{b_l} = \frac{i}{2} \sum_l \langle e^{-i\varphi} b_l^\dagger b_{l-1} - e^{i\varphi} b_{l-1}^\dagger b_l \rangle. \quad (9)$$

So, the chiral current is given by $J = J_a - J_b$. In the single particle ground state when ξ is kept constant, the chiral current increases sinusoidally for increasing magnetic flux upto the critical point (φ_c). On increasing φ beyond the critical point, it starts to decrease suggesting a phase transition from Meissner phase to vortex phase as shown in Fig. 2(a). The same kind of phase transition can be seen on increasing the relative hopping strength

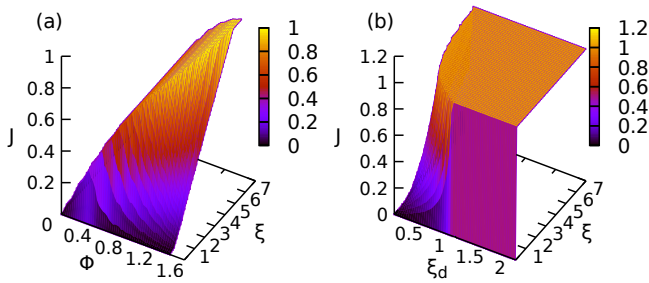


FIG. 2: Variation of chiral current (\mathbf{J}) for one particle ground state with parameters (a) ξ and φ with $\xi_d = 0$, and (b) ξ and ξ_d for a constant $\varphi = \frac{\pi}{2}$.

(ξ) of the ladder for a constant magnetic field, as was reported earlier [1]. The chiral current initially increases with increase in ξ and beyond the critical point (ξ_c) it saturates indicating the vortex-to-Meissner phase transition.

Next we study the entanglement between the two legs of the ladder; in other words, we consider the horizontal division as shown in Fig.1 of the main paper. The vortex-to-Meissner transition is nicely captured at the single particle level. The two-point correlations restricted to the subsystem lattice sites yield the subsystem correlation matrix, from which the entanglement entropy can be computed. The subsystem correlation matrix pertaining to \mathbf{a} is

$$C^{\mathbf{a}} = \left[\frac{1}{L} \sum_k e^{-ik(m-n)} \frac{(\xi + \xi_d \cos k)^2}{N^2} \right]_{L \times L}, \quad (10)$$

where the summation over k is made over all the occupied levels. For single particle ground states, it would just be one number. Fig. 3 shows subsystem entropy behaviour with change in φ and ξ .

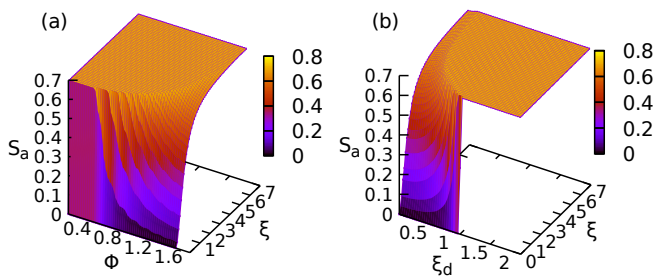


FIG. 3: Entropy of subsystem \mathbf{a} (S_a) of one particle ground state as a function of (a) ξ and φ (b) ξ and ξ_d i.e. diagonal hopping and $\varphi = \frac{\pi}{2}$.

Here, for small φ with constant ξ the system is in the maximally entangled state i.e. an entropy of $\log 2$. This is because for small φ the system has a unique minimum for the lower energy band, which indicates that the particle could be on either of the legs of the ladder with equal probability (Eq.(4) with $\xi_d = 0$), which in turn means

that the entropy is maximal. On increasing φ beyond φ_c there are two degenerate minima for the lower energy band i.e. the particle is either on the upper leg (a) for positive momentum or on the lower leg (b) for negative momentum. Since the lack of information is minimal, this results in low entanglement entropy of the subsystem. Similar behaviour is shown with variation of ξ keeping φ constant. For $\xi = 0$ the two legs are disconnected, and therefore the entanglement entropy for subsystem \mathbf{a} is zero. It increases on increasing ξ till ξ_c . Thereafter, it saturates because the minimum is unique and at $k = 0$ i.e. the maximally entangled state.

B. Diagonal hopping

When diagonal hopping t_d is turned on, the ladder system is rich with multiple phases. First, there is still the vortex to Meissner phase transition. Once again, signatures for this transition are seen both in chiral current shown in Fig. 2(b), and in entanglement entropy for the same conditions as shown in Fig. 3(b). Diagonal hopping favours the Meissner phase as indicated by Eq. 4. It also contributes to making the probability of the particle being in either leg equiprobable in the Meissner phase, and thus making the ground state maximally entangled.

Diagonal hopping also induces a topological phase transition, which is the focus of the main paper. With open boundary conditions (OBC), the energy spectra for a constant ξ and a constant magnetic flux with varying ξ_d is shown in Fig. 4(a). A pair of zero energy states i.e. edge states appear for $\xi_d \geq \xi$ signalling a trivial-to-topological phase transition in the system. We observe that for $\varphi = \frac{\pi}{2}$, the spectrum is symmetric about the zero energy modes. For other φ , the symmetry is broken; however, the topological phase transition always happens at the same point $\xi_d = \xi$, independent of φ . The case $\varphi = \frac{\pi}{2}$ is special. Here, the unitary transformation $U_c = (\sigma_z + \sigma_y)/\sqrt{2}$ applied to eq. 2 yields a structure similar to that of the SSH model. One way to visualize the ladder model as a generalization of the SSH model is as follows. Consider a series of unit cells each consisting of two-sites (one of type ‘a’ and the other of type ‘b’) as shown in Fig. 5(a). If the neighboring unit cells are connected in such a way that only type ‘b’ site of one unit cell couples with type ‘a’ of the neighbouring cell, then the SSH model is obtained (Fig. 5(b)). On the other hand, if every site of a unit cell couples with every site of the neighbouring cell, then the ladder model is obtained. The momentum space Hamiltonian under a suitable unitary transformation yielding a structure identical to that of the SSH model is a further consequence of the special case of $\varphi = \frac{\pi}{2}$. In the SSH model, the wave functions for the two edge states are localized on the ends of the chain. Analogously, in the ladder model, edge states (Figs. 4(b) and 4(c)) are localized on the ends (first and last unit cells) i.e. (a_1, b_1) and (a_L, b_L) and decay exponentially in the bulk. Unlike edge states, any other typical wave

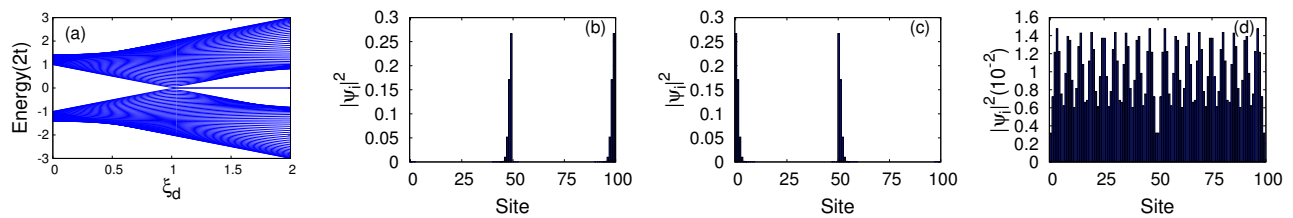


FIG. 4: (a) Energy spectra for ladder system with varying ξ_d . Squared amplitudes of the coefficients of wave function (ψ_i^2) for edge states are shown in (b) and (c), and for a typical bulk state in (d), with ξ_d fixed at 1.5. The other parameters $\xi = 1$, number of rungs $L = 50$, $\varphi = \frac{\pi}{2}$ are common to all figures. The indices first run through 1 to L among the ‘a’ sites, and then again 1 to L , through ‘b’ sites, hence the edge-states show signals at one edge and close to the centre of the figure, which is also an edge of the ladder.

function of the system has some random distribution over all the sites as shown in Fig. 4(d).

Apart from the topological phase transition ξ_d can also trigger the vortex to Meissner phase transition. Below a critical value $\xi_d \leq \xi_{dc}$ in the vortex phase [1], a dense region in the energy spectrum can be discerned. This is a signature of enhanced degeneracy which in turn is a consequence of the presence of two minima (maxima) in the lower (higher) energy band. Beyond ξ_{dc} , in the Meissner phase, energy density is diminished. The critical point ξ_{dc} is the point at which the two minima merge into one, and can be analytically computed for general φ :

$$\xi_{dc} = \begin{cases} \frac{-(\xi + \cos \varphi) + \sqrt{(\xi - \cos \varphi)^2 + 4 \sin^2 \varphi}}{2}, & \xi \leq \frac{\sin^2 \varphi}{\cos \varphi} \\ 0, & \xi \geq \frac{\sin^2 \varphi}{\cos \varphi} \end{cases} \quad (11)$$

Conversely, in terms of ξ_d the critical point ξ_c is given by

$$\xi_c = \begin{cases} \frac{\sin^2 \varphi - \xi_d^2 - \xi_d \cos \varphi}{\xi_d + \cos \varphi}, & \xi_d \leq \frac{-\cos \varphi + \sqrt{1 + 3 \sin^2 \varphi}}{2} \\ 0, & \xi_d \geq \frac{-\cos \varphi + \sqrt{1 + 3 \sin^2 \varphi}}{2} \end{cases}. \quad (12)$$

Eq. (12) shows that the critical point ξ_c decreases on increasing diagonal hopping upto $\xi_d = 1$ as already suggested by a study of chiral current in Fig. 2(b). For $\xi_d \geq 1$, $\xi_c = 0$ because the relative critical value is never negative. A further look at Fig. 4(a) reveals that, there is a reappearance of dense states in the topological region. This is a consequence of degeneracy due to the appearance of two *maxima* (*minima*) in the lower (higher) energy band. This is a new phase transition, different from vortex-Meissner, and appears to have not been reported earlier and has features of a van Hove singularity [3]. This new critical point is given by

$$\xi'_{dc} = \left(\frac{\xi + \sqrt{\xi^2 + 4}}{2} \right)_{\varphi = \frac{\pi}{2}}. \quad (13)$$

We have computed this point, only for the case $\varphi = \frac{\pi}{2}$, where the bandstructure is symmetric (Fig. 4(a)). The maxima of the lower band appear at the zone boundary when $\xi \leq \xi'_{dc}$. But for $\xi_d > \xi'_{dc}$ they start to move

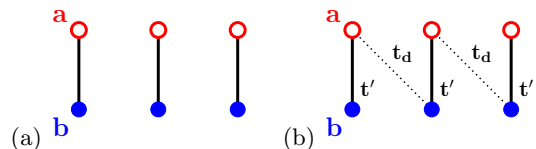


FIG. 5: Visualizing the SSH model as being made up of two-site unit cells.

inside resulting in degeneracy of other eigenstates. The maximum possible shift is $k = \pi/2$, which corresponds to the limit $\xi_d \rightarrow \infty$ when the ladder model behaves as two independent nearest neighbour tight-binding chains.

III. MANY BODY ENTANGLEMENT WITH VERTICAL DIVISION

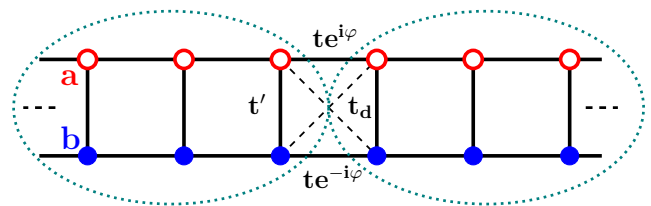


FIG. 6: Ladder system with vertical division of two subsystems.

Another useful division for the purpose of studying entanglement entropy is to consider two subsystems obtained by cutting the ladder vertically as shown in Fig. 6. In the vertical division case, the entanglement entropy seems to be closely correlated with the band spectrum. For $\phi = \pi/2$, the band spectrum is symmetric about the centre, as shown in Fig. 4(a). The band closes at $\xi_d = \xi$ and forms two degenerate edge modes when the boundary conditions are open.

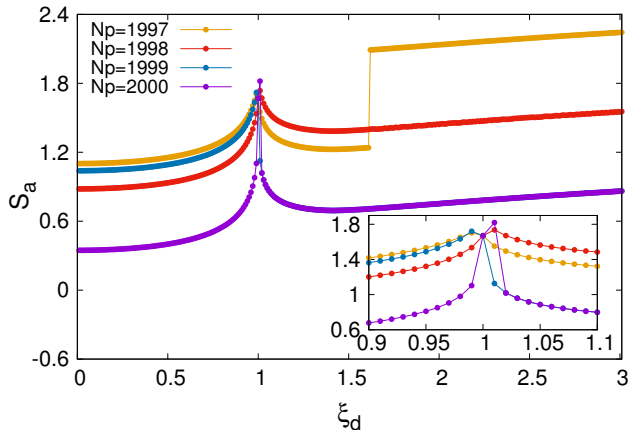


FIG. 7: Subsystem entanglement entropy (S_a) with ξ_d for $L = 1000$, $\xi = 1$, $\varphi = \frac{\pi}{2}$ with open boundary conditions.

When the boundary conditions are closed, the band gap closes at $\xi_d = \xi$, but the gap is non-zero on either side of the topological phase transition. From Fig. 7 and Fig. 8, we observe that at the topological phase transition point, the entanglement entropy takes on the same identical value for a range of fillings close to half-filling. Furthermore, with periodic boundary conditions, the entanglement entropy is maximum at the topological phase transition. The point where entanglement entropy attains a common value for a variety of fillings close to half-filling, and around which it spays out for different fillings, is thus a useful method to capture a topological phase transition. The magnitude of the entanglement here is much smaller than that obtained within horizontal division, because here it is only one (or two in the case of periodic boundary conditions) plaquette that contributes to the entanglement, whereas with horizontal division, every rung contributes, thus making the overall entanglement of the order of the number of particles N_p .

A further feature that entanglement entropy is sensitive to, is the enhanced degeneracy that appears in the band structure at the critical point described by Eq. 13. The sharp increase in density of states might be indicative of a van Hove singularity. A jump in entropy appears when the particle filling is half-filling minus three as shown in Fig. 7 and Fig. 8 both of which have this point at $\xi_d = 1.618$, in agreement with Eq. 13. The reason for this goes back to the argument we employed to reach Eq. 13. When particles are removed starting

from half-filling (which results in only one of the two edge states being occupied), the first particle is removed from the edge state. The next two particles then come off from the maxima in the bands, and then there are four degenerate levels for the next particles. It is at this filling level, with the enhanced degeneracy, that entanglement entropy shows the sensitivity. Once again, calculating

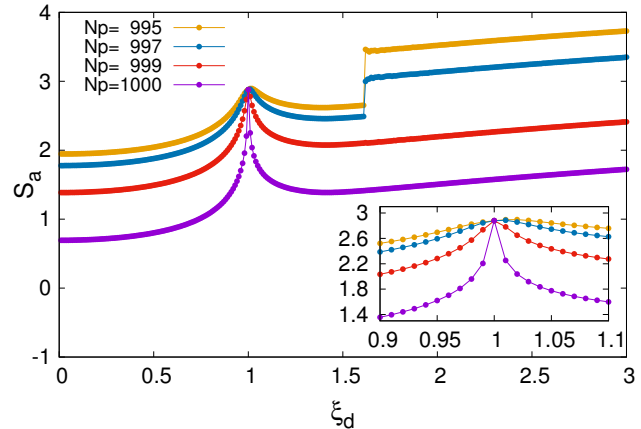


FIG. 8: Subsystem entanglement entropy (S_a) with ξ_d for $L = 1000$, $\xi = 1$, $\varphi = \frac{\pi}{2}$ with periodic boundary conditions.

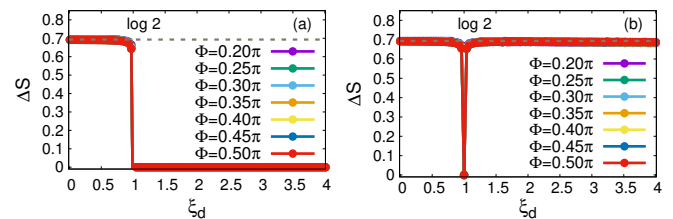


FIG. 9: Subsystem entanglement entropy of ladder system (ΔS_a) with ξ_d . (a) OBC, (b) PBC.

the entanglement entropy difference between half filled and one less than half filled captures the trivial to topological phase transition, as shown in Fig. 9. With open boundary conditions, for ($\xi_d < \xi$), there is a finite value of $\Delta S = \log 2$ whereas after ($\xi_d = \xi$) due to the degeneracy of the edge modes the entropy difference ΔS tends to zero. However, in the case of periodic boundary conditions, the gap is closed only at $\xi_d = 1$, hence the entropy difference goes to zero at that point alone. Once again, we see that this is a feature of the topological phase transition, and is thus completely independent of φ .

[1] D. Hugel and B. Paredes, Physical Review A **89**, 023619 (2014).
 [2] M. Atala, M. Aidelsburger, M. Lohse, J. T. Barreiro, B. Paredes, and I. Bloch, Nature Physics **10**, 588 (2014).

[3] N. W. Ashcroft and N. D. Mermin, Saunders, Philadelphia (1976).